

# Integrative Analysis of the Roles of lncRNAs and mRNAs in Itaconate-Mediated Protection Against Liver Ischemia-Reperfusion Injury in Mice

Yanan Xu<sup>1,\*</sup>

Zihao Li<sup>1,\*</sup>

Shounan Lu<sup>2</sup>

Chaoqun Wang<sup>2</sup>

Shanjia Ke<sup>2</sup>

Xinglong Li<sup>2</sup>

Bing Yin<sup>2</sup>

Hongjun Yu<sup>2</sup>

Menghua Zhou<sup>1</sup>

Shangha Pan<sup>3</sup>

Hongchi Jiang<sup>1</sup>

Yong Ma<sup>2</sup>

<sup>1</sup>Key Laboratory of Hepatosplenic Surgery, Ministry of Education, Department of Hepatic Surgery, The First Affiliated Hospital of Harbin Medical University, Harbin, Heilongjiang Province, People's Republic of China; <sup>2</sup>Key Laboratory of Hepatosplenic Surgery, Ministry of Education, Department of Hepatic Minimal Invasive Surgery, The First Affiliated Hospital of Harbin Medical University, Harbin, Heilongjiang Province, People's Republic of China; <sup>3</sup>Key Laboratory of Hepatosplenic Surgery, Ministry of Education, The First Affiliated Hospital of Harbin Medical University, Harbin, Heilongjiang Province, People's Republic of China

\*These authors contributed equally to this work

Correspondence: Hongchi Jiang; Yong Ma  
Key Laboratory of Hepatosplenic Surgery,  
Ministry of Education, The First Affiliated  
Hospital of Harbin Medical University,  
Harbin, Heilongjiang Province, 150001,  
People's Republic of China  
Tel +86-451-85553886;  
+86-451-85555376  
Email jianghc2013@163.com;  
mayong@ems.hrbmu.edu.cn

**Purpose:** Itaconate is well known for its strong anti-inflammatory and antioxidant effect, but little is known about the potential role of long non-coding RNAs (lncRNAs) in the underlying mechanisms of hepatic ischemia-reperfusion (IR) injury. The aim of our study is to identify lncRNAs related to IR injury and itaconate-mediated protection and to demonstrate the mechanism by which itaconate acts in liver IR injury from the new perspective of lncRNAs.

**Methods:** 4-Octyl itaconate (OI), a membrane-permeable derivative of itaconate, was used as a substitute for itaconate in our study. By using a mouse model of hepatic IR injury, serum and liver samples were collected to measure indexes of liver injury. Then, the liver samples of the mice were subjected to RNA sequencing (RNA-seq) and subsequent bioinformatics analysis.

**Results:** Itaconate attenuated liver IR injury. A total of 138 lncRNAs and 156 messenger RNAs (mRNAs) were markedly differentially expressed in the IR-damaged liver tissues pretreated with OI compared with the matched liver tissues treated with vehicle. Functional analysis indicated that lncRNAs may indirectly participate in the effects of itaconate. Furthermore, 41 mRNAs were examined for the protein-protein interaction (PPI) network analysis, and a key gene cluster was defined. Then, combined the coexpression analysis and the *cis* and *trans* regulatory function prediction of lncRNAs, some "candidate" lncRNA-mRNA pairs which might relate to itaconate-mediated liver protection were identified, while the relationship requires future validation.

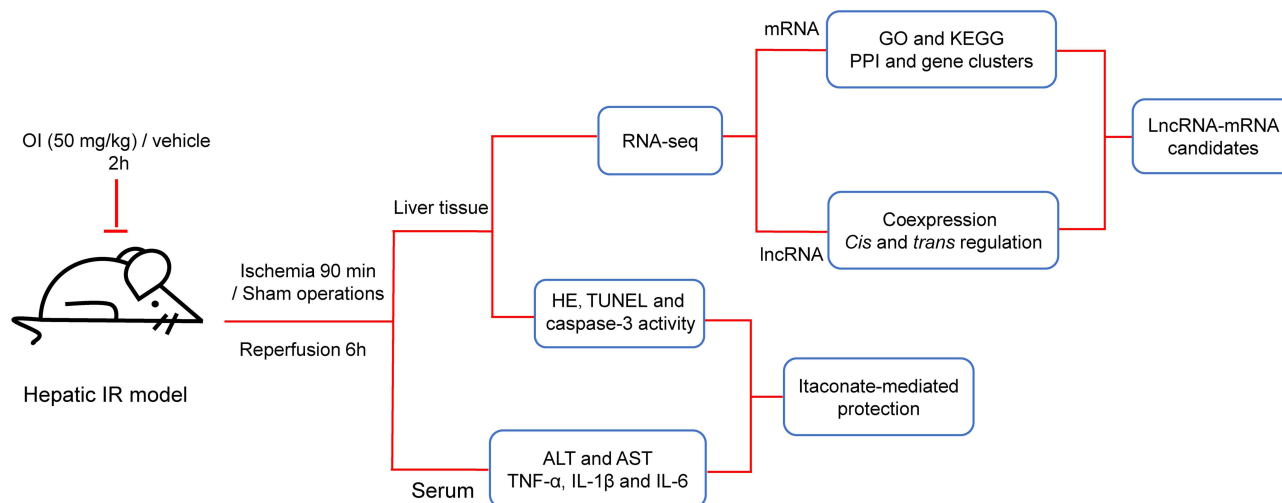
**Conclusion:** Our study revealed that itaconate could protect the liver against IR injury and that lncRNAs might play a role in this process. Our study provides a novel way to investigate the mechanism by which itaconate affects hepatic IR injury and exerts its anti-inflammatory and antioxidative stress effects.

**Keywords:** itaconate, ischemia-reperfusion injury, liver, lncRNA

## Introduction

Liver ischemia-reperfusion (IR) injury is a dynamic process that involves local ischemic injury and inflammation-induced reperfusion insult; it is common in partial hepatectomy, liver transplantation, shock and other serious systemic diseases.<sup>1</sup> Compared with the hepatic parenchymal cell death that occurs during ischemia due to deficient oxygen supply, glycogen depletion and ATP consumption, reperfusion injury is not only a disorder of cell metabolism but also a complex inflammatory immune response. Hepatocytes and nonparenchymal cells (such as Kupffer cells) play an important role in this process.<sup>2-4</sup>

## Graphical Abstract



Itaconate is a metabolite synthesized by the decarboxylation of cis-aconitate in the tricarboxylic acid cycle and plays a vital role in reducing the inflammatory reaction and oxidative stress.<sup>5</sup> Itaconate regulates the interleukin 1 $\beta$  (IL-1 $\beta$ )-hypoxia inducible factor-1 $\alpha$  (HIF-1 $\alpha$ ) axis by inhibiting succinate dehydrogenase (SDH)-mediated succinate oxidation and thus limits the inflammatory response by regulating macrophage metabolic remodeling.<sup>6</sup> In activated macrophages, itaconate can also enhance nuclear factor E2-related factor 2 (Nrf2) levels via alkylation of kelch-like ECH-associated protein 1 (KEAP1) and activate antioxidant and anti-inflammatory programs to inhibit of IL-1 $\beta$  production.<sup>7</sup> In addition, itaconate inhibits hydrogen peroxide-induced oxidative injury by activating Nrf2 signaling cascades to protect osteoblasts.<sup>8</sup> Similarly, in hepatocytes, itaconate can activate the Nrf2-mediated antioxidant response to prevent IR injury in the liver.<sup>9</sup>

Recently, an increasing number of long non-coding RNAs (lncRNAs) have been detected, so an increasing number of researches have focused on investigating the role of lncRNAs in liver IR injury. Some well-known lncRNAs have been confirmed to be involved in liver IR injury. For example, lncRNA HOX transcript antisense RNA (HOTAIR) can regulate autophagy through the miR-20b-5p/ autophagy related 7 (ATG7) axis in liver IR insult.<sup>10</sup> In addition, maternally expressed gene 3 (MEG3) protects hepatocytes from IR insult by downregulating the expression of miR-34a.<sup>11</sup> Moreover, some novel lncRNAs have also been identified and proven to

regulate liver IR injury. For instance, silencing of lncRNA AK139328 attenuates liver IR injury via activating the Akt signaling pathway and inhibiting the nuclear transcription factor kappa B (NF- $\kappa$ B) activity,<sup>12</sup> furthermore, lncRNA AK054386 can act as a competing endogenous RNA to sequester miR-199a-5p and inhibit endoplasmic reticulum stress during liver IR injury.<sup>13</sup>

Despite the lack of experimental verification, RNA sequencing (RNA-Seq) and bioinformatics analysis provide clues for subsequent experimental research, and inspire novel hypotheses.<sup>14</sup> To date, there are very few studies on the expression profiles of lncRNAs in liver IR injury,<sup>12,15</sup> and no studies on the expression profiles of lncRNAs in itaconate-mediated protection on liver IR injury. Therefore, we want to explore whether lncRNA is an important target for itaconate-mediated protection on liver IR injury and conduct further studies. Previous studies have reported that itaconate cannot be taken up by cells and, similarly, that its derivative, dimethyl itaconate, cannot be metabolized into itaconate and cannot accumulate intracellularly in the form of itaconate.<sup>16</sup> However, 4-octyl itaconate (OI), a cell-permeable derivative of itaconate, overcomes these limitations<sup>7</sup> and is a suitable surrogate for investigating the role of itaconate in the context of liver IR injury. Using a mouse model of partial liver IR injury, we confirmed that itaconate could play a protective role during hepatic IR injury in mice. Furthermore, RNA-seq and subsequent bioinformatics analysis were combined to identify lncRNAs related to

hepatic IR injury and itaconate-mediated protection and to demonstrate the mechanism by which itaconate acts in liver IR injury from the new perspective of lncRNAs.

## Materials and Methods

### Animals and Animal Treatment

Male C57BL/6 mice (19–23 g), aged 8 weeks, were purchased from Charles River Lab Animal Center (Beijing, China). All the animals were housed in ventilated cages with five mice per cage at the specific pathogen-free (SPF) facility of the Molecular Biology Centre of the Fourth Affiliated Hospital, Harbin Medical University. The mice were given free access to a normal chow diet and water. Then the mice were randomly divided into four groups, named IR OI group, IR Con group, Sham OI group, and Sham Con group, respectively. The mice in the IR OI group were given an intraperitoneal injection of OI (MCE, Shanghai, China) (50 mg/kg) in 40% solution of (2-hydroxypropyl)- $\beta$ -cyclodextrin (MCE) 2 hours before the operation of hepatic ischemia; the IR Con group were treated intraperitoneally with vehicle 2 hours before the onset of hepatic ischemia. Sham groups involved administration of OI or vehicle, laparotomy and exposure of the portal triad without hepatic ischemia. There are 5–7 mice in each group. The ischemic liver lobe of all mice in the IR groups had visible color changes and no mice died during the liver IR. Serum and liver samples were collected 6 hours after reperfusion for further study. All experiments involving animals were conducted according to the ethical policies and procedures approved by the Institutional Animal Care and Use committee of Harbin Medical University (No. LC2018037) and were conducted according to the Care and Use of Laboratory Animals (Bethesda, MD: National Institutes of Health, 1985).

### Hepatic IR Model

The hepatic IR procedures have been mentioned previously.<sup>17</sup> Briefly, the mice were anesthetized by intraperitoneal injection of 2% sodium pentobarbital (60 mg/kg), and a midline laparotomy was performed. Then, the left lateral and median lobes of the liver were clamped at its base with an atraumatic clip. Throughout anesthesia, the body temperature was maintained at 37°C with a heat lamp. After 90 minutes of ischemia, the clip was removed, initiating hepatic reperfusion.

### Measurement of Serum Parameters

The levels of serum alanine aminotransferase (ALT) and aspartate aminotransferase (AST) were measured with specific assay kits (Nanjing Jiancheng Bioengineering Institute, Nanjing, China). The serum levels of tumor necrosis factor- $\alpha$  (TNF- $\alpha$ ), interleukin 6 (IL-6) and interleukin 1 $\beta$  (IL-1 $\beta$ ) were assessed with ELISA kits (SAB, Maryland, USA). All procedures were performed according to the manufacturer's instructions.

### Histological Analysis

Liver specimens were fixed in 4% paraformaldehyde, embedded in paraffin, stained with hematoxylin and eosin, and examined with a light microscope. The histopathological scoring analysis was performed blindly as previously mentioned.<sup>18</sup>

### Terminal dUTP Nick-End Labeling (TUNEL) Assay

The methodology has been described earlier.<sup>18</sup> TUNEL (Roche, Shanghai, China) staining of the live sections was performed according to the manufacturer's instructions, and the TUNEL-positive cells in ten randomly selected high-power fields were counted under microscopy and are expressed as a percentage of the total hepatocytes.

### Caspase-3 Activity Assay

Caspase-3 activity was performed using Caspase-3 Cellular Activity Assay Kit (Calbiochem, CA, USA), as described previously.<sup>19</sup> Liver samples were used according to the manufacturer's instruction.

### High-Throughput Sequencing Analysis

High-throughput sequencing was performed by Annoroad Gene Technology Corporation (Beijing, China). RNA sample extraction and quality control, library construction and purification, library quality assessment and quantification, cluster generation and sequencing analysis were carried out on the obtained liver tissues. Each step of the experimental process was strictly quality-controlled, and the resulting libraries were sequenced on a Novaseq instrument. An Agilent 2100 RNA Nano 6000 Assay Kit (Agilent Technologies, CA, USA) was used for RNA quality control. Ribo-Zero™ GoldKits (mouse) was used for rRNA removal. The NEB Next Ultra Directional RNA LibraryPrep Kit for Illumina (NEB, Ipswich, USA) and QiaQuick PCR kit were used for library construction and

purification. An Agilent 2100 system (Agilent Technologies, CA, USA) and qPCR analysis (Kapa Biosystems, Woburn, MA, USA) were used for library quality assessment and quantification. TruSeq PE Cluster Kit V4 (Illumina, San Diego, CA, USA) was used for cluster generation. DESeq (<http://www.bioconductor.org/packages/release/bioc/html/DESeq.html>) was used to analyze the differential expression between groups (five biological replicates per group). Significantly differentially expressed genes between two groups were identified using fold change  $\geq 2.0$  and P value  $\leq 0.05$  as the screening indices.

## Functional Analysis

Gene Ontology (GO)<sup>20</sup> can annotate the function of genes from biological process, cellular component and molecular function. Kyoto Encyclopedia of Genes and Genomes (KEGG)<sup>21</sup> focuses on metabolic pathways related to genes. Both of these approaches are used for gene function analysis. We uploaded the differentially expressed messenger RNAs (mRNAs) to the Database for Annotation, Visualization and Integrated Discovery (DAVID).<sup>22</sup> Choosing a P-value  $\leq 0.05$  as the threshold, we used the top ten GO terms and pathways to plot the charts or listed all the GO terms or pathways if their number was less than ten. The results were visualized by an online platform (<http://www.bioinformatics.com.cn>).

## Protein-Protein Interaction (PPI) Network Analysis and Gene Cluster Identification

We applied the Search Tool for the Retrieval of Interacting Genes (STRING)<sup>23</sup> to perform the PPI network analysis of the selected mRNAs and set a combined score  $> 0.4$  as the cutoff point. Cytoscape software<sup>24</sup> was used to dispose the mRNA-mRNA pairs for visualization. Moreover, we used the Molecular Complex Detection (MCODE) plug-in embedded in Cytoscape to identify the key gene clusters in the network (parameters: Degree Cutoff: 2, Haircut, Node Score Cutoff: 0.2, K-Core: 2 and Max. Depth: 100.).

## Coexpression Analysis

On the basis of the Pearson correlation analysis, we evaluated the coexpressed relationship between significantly differentially expressed lncRNAs and mRNAs. Pearson correlation coefficient (PCC)  $\geq 0.70$  and  $P < 0.05$  were determined to be the criteria for further investigation. TBtools software<sup>25</sup> was used to show the top 500 coexpressed lncRNA-mRNA pairs.

## Cis and Trans Regulatory Mechanism Prediction

*Cis* regulation is based on the relationship between the positions of lncRNAs and mRNAs, and the protein-coding genes within 300 kb upstream and downstream of lncRNAs were identified as potential targets. For *trans* prediction, RIsSearch-2.0 software<sup>26</sup> was used to predict the binding of coexpressed lncRNAs and mRNAs at the level of nucleic acid. The number of bases required for a direct interaction between two nucleic acids  $\geq 10$  and the free energy of base binding  $\leq -100$  were chosen as the selection criteria, and the identified lncRNA-mRNA pairs may have a *trans* regulatory relationship. The lncRNA-mRNA regulatory relationship was visualized by Cytoscape software.

**Table 1** Primer Sequences Used to Validate lncRNA and mRNA Expression

Gene	Primer Type	Primer Sequence
MSTRG.19961	Forward primer	GTGAGGTA CTGTGGCAAGC
	Reverse primer	CCAAGTGCTGGGATTAACGG
Gm45301	Forward primer	TGCTCCACATGAGGGCTAAA
	Reverse primer	GCTCTGCTGACTGTTGGAAG
Ptx2	Forward primer	CGGACTGGATTCTATGGTGAAA
	Reverse primer	CTTGAAGTGGGT CAGGATGTAG
Cd3	Forward primer	GAAGATTCCACGCCAATTCATC
	Reverse primer	GATCTGCCGTTTCTCTTAGTC
Gapdh	Forward primer	AGGTCGGTGTGAACGGATTG
	Reverse primer	GGGGTCGTTGATGGCAACA

**Abbreviations:** lncRNA, long non-coding RNA; mRNA, messenger RNA; Ptx2, prostaglandin-endoperoxide synthase 2; Cd3, chemokine (C-C motif) ligand 3; Gapdh, glyceraldehyde-3-phosphate dehydrogenase.

## Real-Time Quantitative Reverse Transcription Polymerase Chain Reaction (qRT-PCR)

Differentially expressed genes were selected, and the obtained sequences were used to design primers for the further verification of these lncRNAs and mRNAs by real-time qRT-PCR. Glyceraldehyde 3-phosphate dehydrogenase (*Gapdh*) was chosen as the internal control. Quantitative differential expression was calculated according to the  $2^{-\Delta\Delta Ct}$  method. All the primer sequences are shown in Table 1.

## Statistical Analysis

Quantitative data were expressed as the mean values  $\pm$  SDs. Comparisons among multiple groups were made with one-way analysis of variance followed by Dunnett *t*-test. The data were statistically analyzed and visualized by GraphPad Prism software.  $P < 0.05$  was considered to be statistically significant.

## Results

### Itaconate-Mediated Protection Against Hepatic IR Injury in Mice

To verify the effect of itaconate on liver IR injury in a mouse model, we collected serum and liver samples and measured indexes of liver injury. As shown in Figure 1A and B, OI treatment did not affect the aminotransferase levels in the sham groups, while this parameter was markedly increased ( $P < 0.05$ ) in the IR groups, compared with the Sham Con group. More importantly, OI pretreatment significantly reduced the ALT (Figure 1A) and AST (Figure 1B) levels induced by IR injury ( $P < 0.05$ ). We measured the levels of TNF- $\alpha$  (Figure 1C), IL-1 $\beta$  (Figure 1D) and IL-6 (Figure 1E) from the four groups as well. Compared with the sham treatment, liver IR injury markedly increased the levels of these cytokines ( $P < 0.05$ ) (Figure 1C–E). OI pretreatment attenuated the increases in the three parameters observed in the IR OI group to levels markedly lower than those in the IR Con group ( $P < 0.05$ ) (Figure 1C–E).

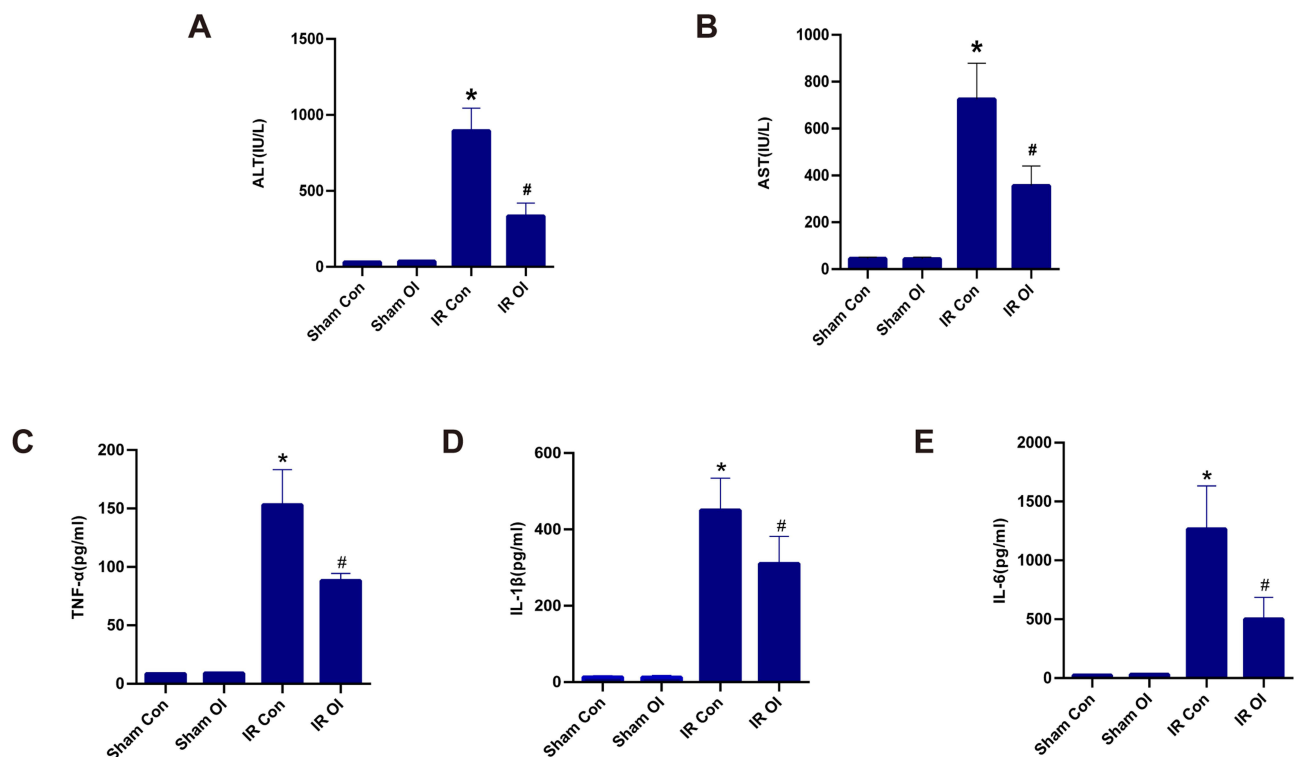


**Figure 1** Itaconate-mediated protection against liver IR injury in mice. The levels of ALT (A) and AST (B) in sera were measured by specific assay kits after 90-minute ischemia and 6-hour reperfusion in the Sham Con, Sham OI, IR Con and IR OI group. TNF- $\alpha$  (C), IL-1 $\beta$  (D) and IL-6 (E) levels were assessed by ELISA. The results are expressed as the mean  $\pm$  SD of 5–7 animals per group. \*Significant difference from the Sham Con group,  $P < 0.05$ . #Significant difference from the IR Con group,  $P < 0.05$ . **Abbreviations:** IR, ischemia-reperfusion; ALT, alanine aminotransferase; AST, aspartate aminotransferase; OI, 4-octyl itaconate; TNF- $\alpha$ , tumor necrosis factor- $\alpha$ ; IL-1 $\beta$ , interleukin 1 $\beta$ ; IL-6, interleukin 6; ELISA, enzyme linked immunosorbent assay; SD, standard deviation.

Furthermore, we observed histopathological changes in hematoxylin-eosin (HE)-stained liver sections, and these changes were consistent with the serological changes. The sham groups treated with OI or vehicle exhibited normal

morphology, showing that itaconate had no effect on liver histology (Figure 2A). The IR Con group showed distinct histological alterations characterized by focal necrosis, hemorrhagic changes and inflammatory cell infiltration,

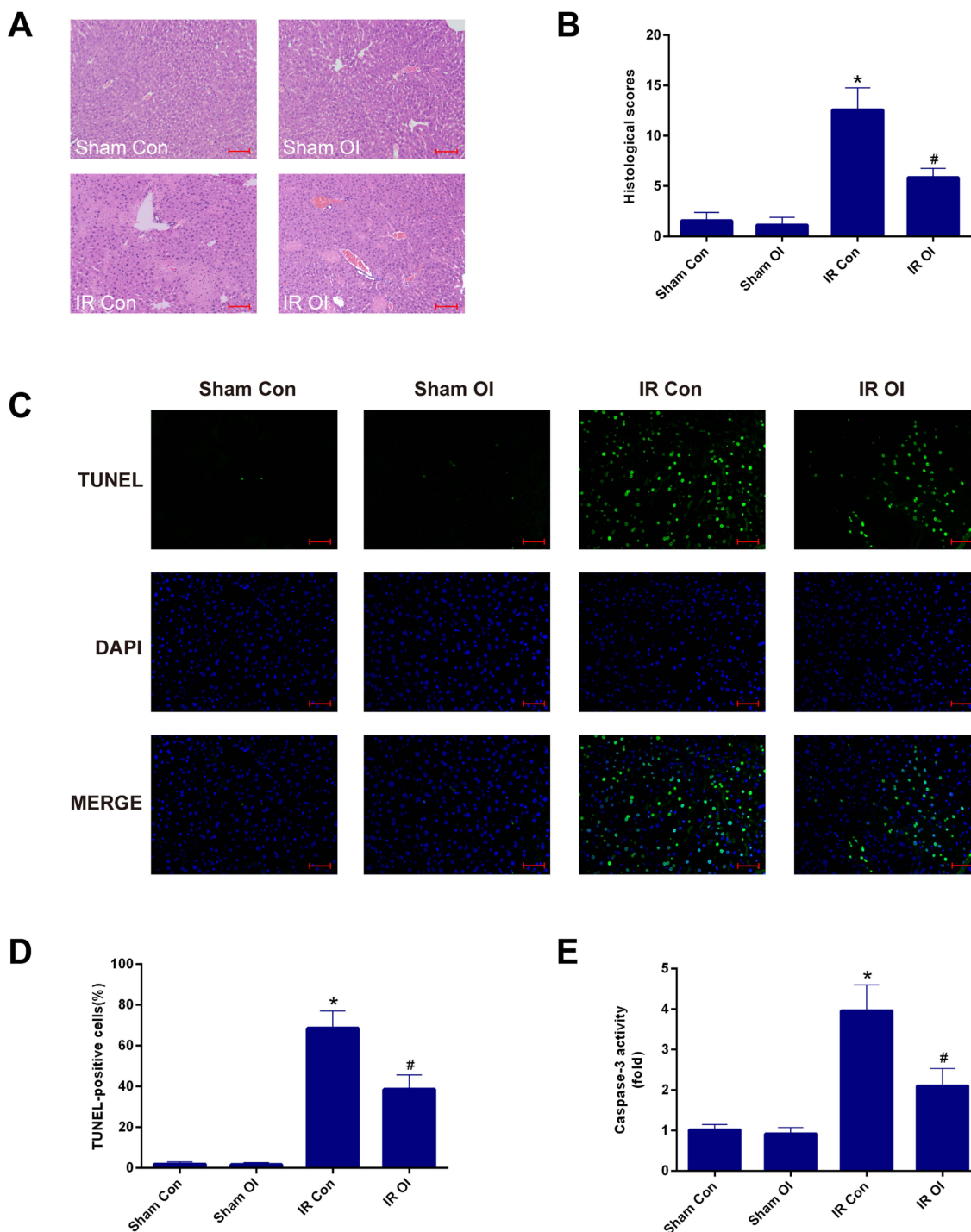


**Figure 2** Itaconate pretreatment attenuates the liver IR injury in mice. **(A)** Representative HE-stained photographs (200×) of liver sections were selected from four groups. **(B)** Histopathological score of hepatic damage was calculated. **(C)** Representative photographs (200×) of liver sections stained by TUNEL were presented from four groups. **(D)** TUNEL-positive cells were counted as described in Materials and methods. **(E)** Caspase-3 activity in the liver tissues was assessed by specific assay kit. Data are showed as mean ± SD of 5–7 animals per group. \*Significant difference from the Sham Con group, P < 0.05. #Significant difference from the IR Con group, P < 0.05. Bar: 100 μm. **Abbreviations:** IR, ischemia-reperfusion; HE, hematoxylin-eosin; TUNEL, terminal dUTP nick-end labeling; SD, standard deviation; DAPI, 4',6-diamidino-2-phenylindole.

and by comparison, pretreatment with OI significantly attenuated these histopathological changes (Figure 2A). The liver injury scores of the IR groups were markedly higher than those of the sham operation groups ( $P < 0.05$ ) (Figure 2B), and compared with the control, injection with OI significantly reduced the increased histological scores caused by IR injury ( $P < 0.05$ ) (Figure 2B). Simultaneously, to assess cellular necrosis and apoptosis, we performed TUNEL staining. The results of representative images and positive cell count analysis are displayed in Figure 2C and D. There were few TUNEL-positive cells in the sham groups (Figure 2D); however, liver IR increased the percentage of positive cells to  $68.52\% \pm 8.39\%$ , and this percentage was decreased to  $38.51\% \pm 7.01\%$  by OI administration ( $P < 0.05$ ) (Figure 2D). An increase in caspase-3 activity were observed in the IR groups and OI significantly inhibited the increase, which was consistent with the results of TUNEL (Figure 2E).

## Differentially Expressed lncRNA and mRNA Profiles

We performed RNA-seq on the mouse liver tissues from the four groups. For convenience, we regrouped these mice into four groups to compare the differentially expressed genes and named these groups IR Con vs Sham Con, IR OI vs IR Con, IR OI vs Sham OI, and Sham OI vs Sham Con; in these groupings, the latter samples acted as controls for the former samples. Fold change  $\geq 2.0$  and P value  $\leq 0.05$  served as the screening conditions to screen out the significantly differentially expressed lncRNAs and mRNAs in each comparison group (Table 2). Hierarchical clustering analysis was applied to visualize the lncRNA and mRNA profiles, and heatmaps were constructed, as shown in Figures 3A-D and 4A-D.

Since we were more interested in the mechanism underlying the itaconate-mediated protection against hepatic IR injury, we focused on the changes in lncRNAs and mRNAs after hepatic IR injury and after OI pretreatment. As shown in Table 2, there were 266 upregulated and 239 downregulated lncRNAs and 640 upregulated and 248 downregulated mRNAs in the IR Con vs Sham Con group. Additionally, there were 60 upregulated and 78 downregulated lncRNAs and 36 upregulated and 120 downregulated mRNAs in the IR OI vs IR Con group (Table 2). Here, we also showed the top five significantly upregulated and downregulated lncRNAs and mRNAs in the IR OI vs IR Con group (Tables 3 and 4).

## Functional Analysis of the Differentially Expressed Genes

Although lncRNAs cannot encode genes, they can regulate gene expression, and changes in gene expression can, in turn, indirectly reflect the function of lncRNAs. Therefore, we performed functional analysis of markedly upregulated and downregulated mRNAs to gain a preliminary understanding of the potential function of the differentially expressed lncRNAs. As shown in Figure 5A, it seems that the protective role of itaconate mostly occurs by downregulating mRNAs. These mRNAs, which were mainly located in the extracellular region, participated in the inflammatory response, immune response, cellular response to cytokines, inflammatory cells and immune cell chemotaxis. In the molecular function domain, these mRNAs primarily participated in cytokine activity, chemokine activity, growth factor activity and chemokine receptor binding (Figure 5A). These results were similar to those of the mRNAs that were upregulated after liver IR injury (Figure 5B). In addition, the downregulated genes after liver IR injury were mostly located in the

**Table 2** Number of Significantly Differentially Expressed Genes in Each Comparison Group

Comparison Group	Class	Upregulated	Downregulated	Total
IR Con vs Sham Con	lncRNA	266	239	505
IR OI vs IR Con	lncRNA	60	78	138
IR OI vs Sham OI	lncRNA	248	288	536
Sham OI vs Sham Con	lncRNA	105	79	184
IR Con vs Sham Con	mRNA	640	248	888
IR OI vs IR Con	mRNA	36	120	156
IR OI vs Sham OI	mRNA	387	275	662
Sham OI vs Sham Con	mRNA	108	106	214

**Abbreviations:** IR, ischemia-reperfusion; lncRNA, long non-coding RNA; OI, 4-octyl itaconate; mRNA, messenger RNA.

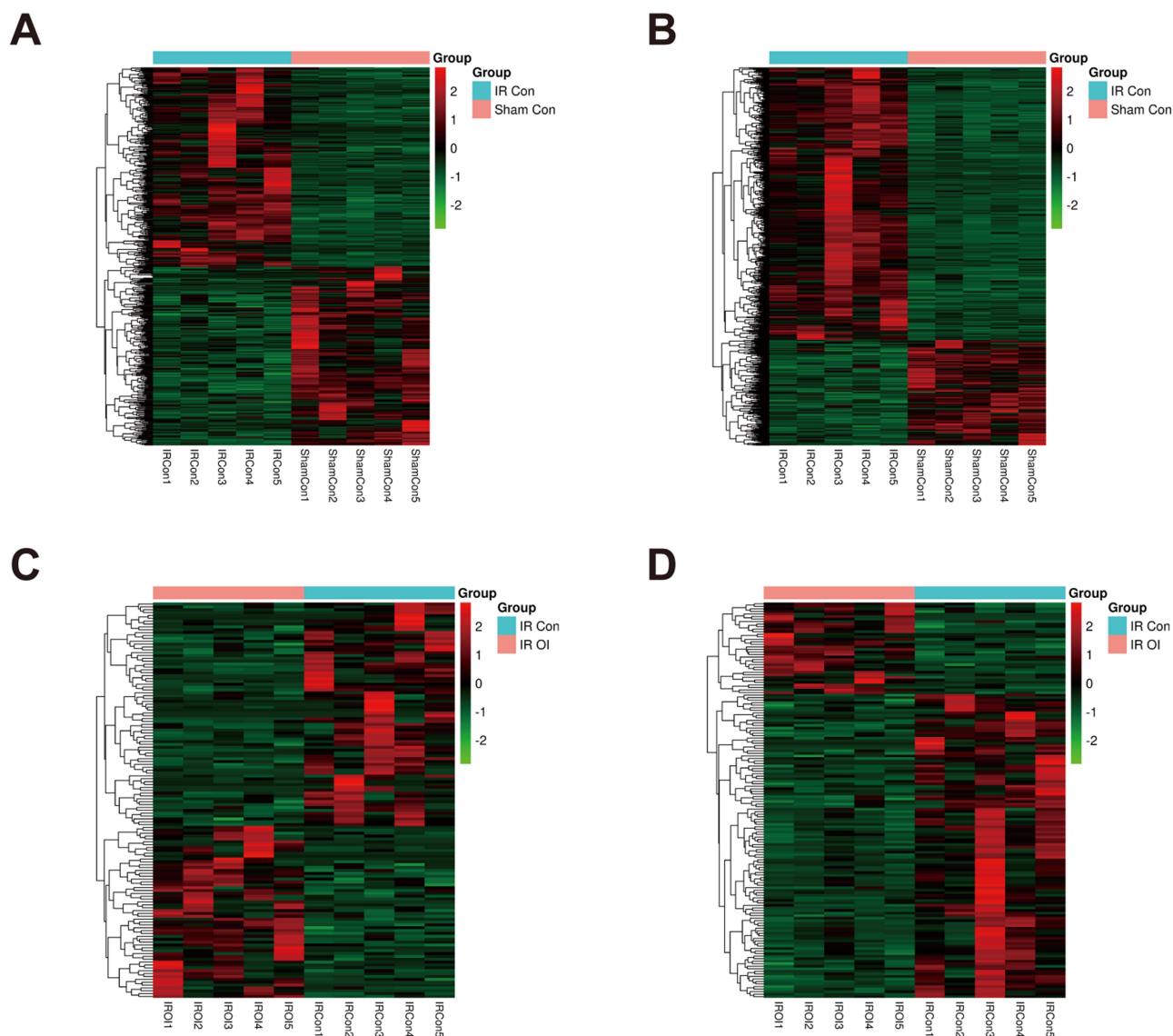


**Figure 3** lncRNA and mRNA expression profiles after hepatic IR injury and after OI pretreatment. Heatmaps were drawn to show the results of hierarchical clustering analysis for the differentially expressed genes, fold change  $\geq 2.0$  and P value  $< 0.05$  as the filtering criteria. **(A and B)** are showed lncRNA and mRNA expression profiles of the IR Con vs Sham Con group, **(C and D)** displaying differentially expressed lncRNAs and mRNAs of the IR OI vs IR Con group, respectively. The color scale represents the variation of expression values. Green indicates low expression and red indicates high expression.

**Abbreviations:** lncRNA, long non-coding RNA; mRNA, messenger RNA; IR, ischemia-reperfusion; OI, 4-octyl itaconate.

extracellular region and membrane structure and were associated with enzyme activity (Figure 5C), while the number of GO terms enriched by the genes that were upregulated after OI treatment was low (Figure 5D).

In the KEGG analysis, we found that 47 pathways were significantly enriched in the upregulated mRNAs after liver IR injury and 18 pathways were enriched in the downregulated mRNAs after OI treatment, and we identified the top ten pathways (Figure 6A and B). There were 14 identical pathways, such as malaria, TNF signaling pathway, Salmonella infection, and rheumatoid arthritis (Table 5).

As shown in Figure 6C and D, there were 6 pathways related to the downregulated mRNAs after IR injury and the upregulated mRNAs after OI administration; among these pathways, both the PPAR signaling pathway and retinol metabolism were related to both groups of mRNAs.

### PPI Network Construction and Gene Cluster Analysis

To further identify the lncRNAs possibly associated with the function of itaconate, we emphasized 41 mRNAs that were simultaneously differentially expressed only in both



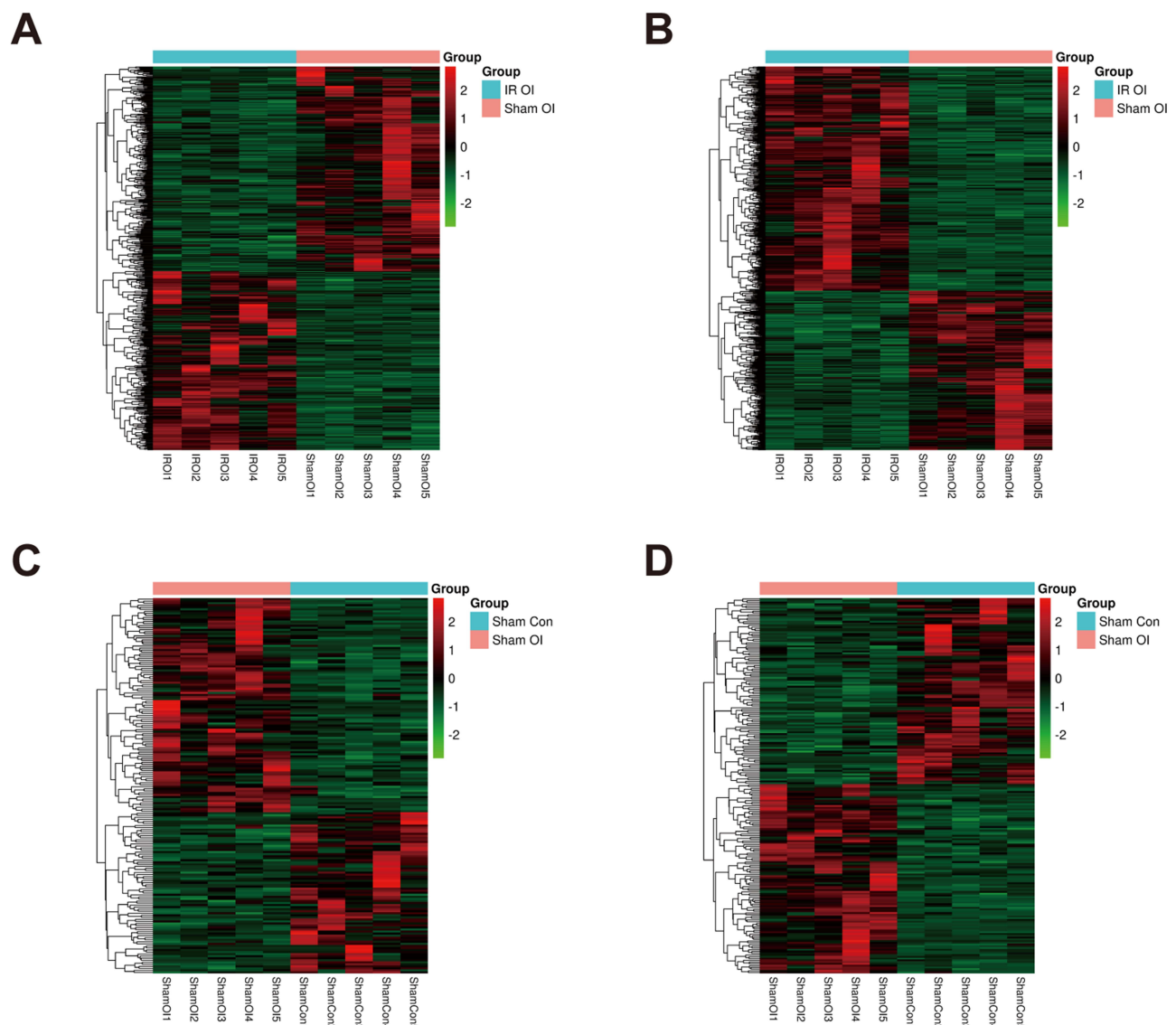


**Figure 4** lncRNA and mRNA expression profiles in the IR OI vs Sham OI and the Sham OI vs Sham Con group. Heatmaps were drawn to show the results of hierarchical clustering analysis for the differentially expressed genes, fold change  $\geq 2.0$  and P value  $< 0.05$  as the filtering criteria. **(A and B)** are showed lncRNA and mRNA expression profiles of the IR OI vs Sham OI group, **(C and D)** displaying differentially expressed lncRNAs and mRNAs of the Sham OI vs Sham Con group, respectively. The color scale represents the variation of expression values. Green represents low expression and red represents high expression.

**Abbreviations:** lncRNA, long non-coding RNA; mRNA, messenger RNA; IR, ischemia-reperfusion; OI, 4-octyl itaconate.

the IR Con vs Sham Con group and the IR OI vs IR Con group (Figure 7A). Most of these differentially expressed mRNAs were upregulated after liver IR injury but downregulated after OI pretreatment before liver IR injury (Figure 7B). These 41 mRNAs were examined to construct the PPI network using the STRING database, which consisted of 24 nodes and 46 edges (Figure 7C). Using the plugin “MCODE”, we identified a significant gene cluster (score: 6.571) in this PPI network. There were eight identified genes, namely, interleukin 6 (*Il6*), interleukin 1 beta (*Il1b*), prostaglandin-endoperoxide synthase 2 (*Ptgs2*), matrix metalloproteinase 13 (*Mmp13*),

chemokine (C-C motif) ligand 3 (*Ccl3*), chemokine (C-C motif) ligand 4 (*Ccl4*), oncostatin M (*Osm*), and interleukin 1 family, member 9 (*Il1f9*) and 23 edges (Figure 7D).

### Cis and Trans Regulatory Function Prediction of lncRNAs

Furthermore, we performed Pearson correlation analysis on all the markedly differentially expressed lncRNAs and mRNAs in the IR OI vs IR Con group and selected PCC  $\geq 0.70$  and P  $< 0.05$  as the thresholds. We identified 2874

**Table 3** The Top Five Upregulated and Downregulated lncRNAs in the IR OI vs IR Con Group

lncRNA	Regulation	Log2 FC	P-value	Chr	Strand
MSTRG.71622	Up	4.019809821	0.004781685	3	+
MSTRG.77804	Up	3.940331445	0.006558533	4	-
MSTRG.81818	Up	3.85884802	0.004975173	4	+
MSTRG.19646	Up	3.237892789	0.041562274	11	+
MSTRG.66533	Up	2.922372056	0.016237046	2	+
MSTRG.95431	Down	-4.091151015	0.001598667	6	+
Gm2511	Down	-4.053316967	0.001985725	7	-
MSTRG.44046	Down	-3.773367156	0.012606973	16	+
MSTRG.95095	Down	-3.705136963	0.010920314	6	-
MSTRG.112518	Down	-3.684913095	0.013508003	9	-

**Abbreviations:** lncRNAs, long non-coding RNAs; IR, ischemia-reperfusion; OI, 4-octyl itaconate; FC, fold change.

**Table 4** The Top Five Upregulated and Downregulated mRNAs in the IR OI vs IR Con Group

mRNA	Regulation	Log2 FC	P-value	Chr	Strand
<i>Hsd17b14</i>	Up	3.41456671	0.021101567	7	+
<i>Mesp2</i>	Up	2.754709071	0.016055081	7	+
<i>Mybpc3</i>	Up	2.483217871	0.040256373	2	+
<i>Cux2</i>	Up	2.247214652	0.003997402	5	-
<i>Anxa8</i>	Up	2.245431703	0.031322302	14	+
<i>Ccl19</i>	Down	-4.540876959	0.000108196	4	-
<i>Chrne</i>	Down	-3.348936056	0.023273987	11	-
<i>Grem1</i>	Down	-3.275591963	0.038552212	2	-
<i>Armc12</i>	Down	-3.261208193	0.038625845	17	+
<i>Gm4131</i>	Down	-3.26075815	0.038512268	14	-

**Abbreviations:** mRNAs, messenger RNAs; IR, ischemia-reperfusion; OI, 4-octyl itaconate; FC, fold change; *Hsd17b14*, hydroxysteroid (17-beta) dehydrogenase 14; *Mesp2*, mesoderm posterior 2; *Mybpc3*, myosin binding protein C3; *Cux2*, cut-like homeobox 2; *Anxa8*, annexin A8; *Ccl19*, chemokine (C-C motif) ligand 19; *Chrne*, cholinergic receptor, nicotinic, epsilon polypeptide; *Grem1*, gremlin 1; *Armc12*, armadillo repeat containing 12.

lncRNA-mRNA pairs, most of which (2421/2874) were positively correlated, and the rest (453/2874) were negatively correlated. A Circos map was drawn to display the top 500 lncRNA-mRNA pairs (Figure 8A). Based on the results of the coexpression analysis, the *cis* and *trans* regulatory mechanisms of the lncRNAs was predicted, and the results were as follows.

We searched the adjacent coding genes of each lncRNA (within 300 kb on the same chromosome) and identified five pairs of regulatory relationships (Figure 8B). lncRNA MSTRG.19961 might *cis*-regulate *Ccl3* (251397bp, PCC = -0.79633184) and *Ccl4* (266137bp, PCC = -0.714979773), which were identified above (Figure 8C). For the prediction of *trans* regulatory mechanisms, we used RNA interaction software to predict the potential binding of lncRNAs and mRNAs at the level of nucleic acid. A total of 413 lncRNA-mRNA pairs that may have direct regulatory mechanisms were identified (Figure 8D). lncRNA Gm16045 was found

to have 31 potential *trans*-targeted genes including *Osm* and *Il19f*. In addition, *Il6* and *Ccl4* were *trans*-regulated by lncRNA D330050G23Rik, and *Ptgs2* was *trans*-regulated by lncRNA Gm45301. lncRNA MSTRG.15746 and *Il6* as well as lncRNA MSTRG.74451 and *Il1f9* may have *trans*-regulatory relationships (Figure 8D). These results suggested that lncRNAs and their targeted genes might be associated with the protective effect of itaconate, indicating that the regulatory role of lncRNAs is an ideal entry point to study the mechanism by which itaconate alleviates liver IR injury.

### Validation of Gene Expression Using qRT-PCR

To validate the reliability of the sequencing results, some lncRNAs and mRNAs were chosen for qRT-PCR analysis. The qRT-PCR results indicated that the expression of lncRNA MSTRG.19961 was upregulated (Figure 9A)

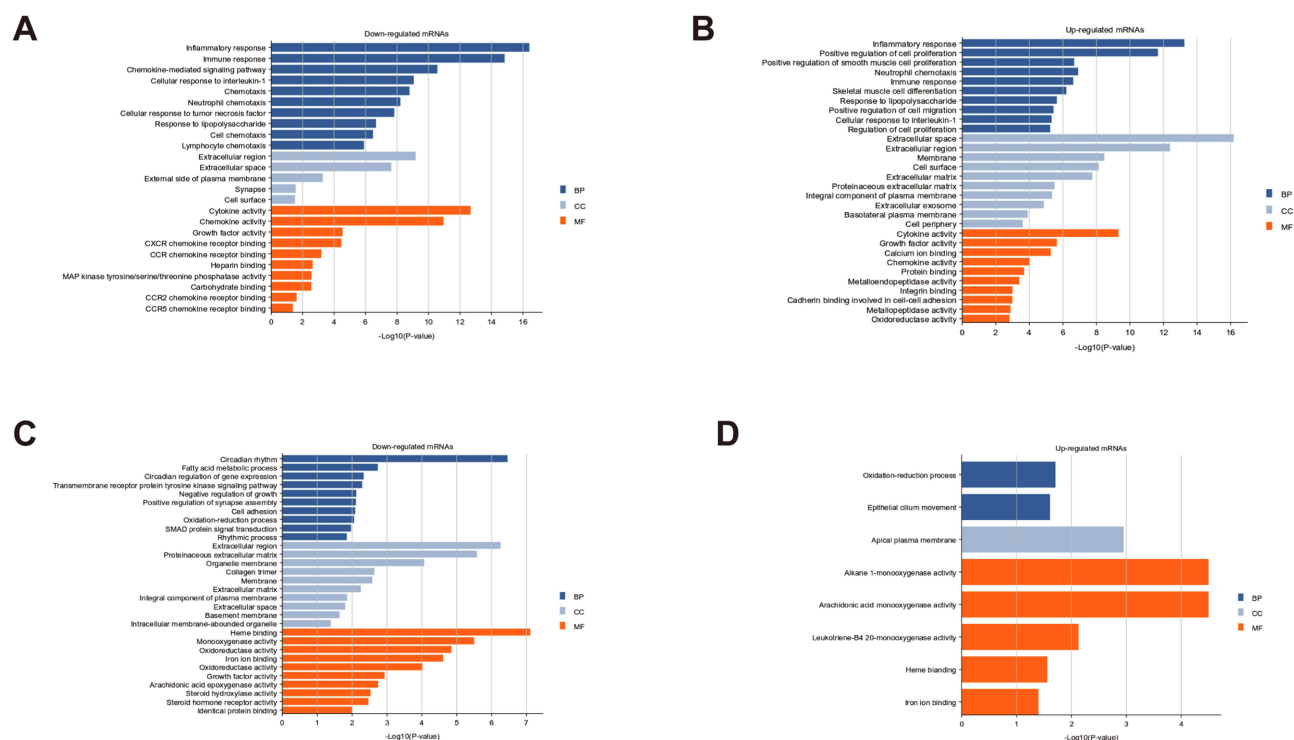


**Figure 5** GO analysis of significantly differentially expressed mRNAs. GO terms of upregulated and downregulated mRNAs in the IR Con vs Sham Con group and the IR OI vs IR Con group. **(A)** Downregulated mRNAs after OI pretreatment. **(B)** Upregulated mRNAs after hepatic IR injury. **(C)** Downregulated mRNAs after hepatic IR injury. **(D)** Upregulated mRNAs after OI pretreatment. The top ten or all the GO terms with P value < 0.05 were listed.

**Abbreviations:** GO, Gene Ontology; mRNAs, messenger RNAs; IR, ischemia-reperfusion; OI, 4-octyl itaconate; BP, biological process; CC, cellular component; MF, molecular function.

and the expression of Gm45301 was downregulated (Figure 9B) in the IR OI vs IR Con group. Two mRNAs, *Ptgs2* (Figure 9D) and *Ccl3* (Figure 9E), were upregulated in the IR Con vs Sham Con group and downregulated in the IR OI vs IR Con group, whereas they were not significantly different in the other two comparison groups. These results were consistent with our sequencing results (Figure 9C and F).

## Discussion

Itaconate did not receive much attention until its strong anti-inflammatory effect through the regulation of macrophage metabolic remodeling was revealed. Studies of itaconate, an immunometabolite, have been focused on the elucidation of its anti-inflammatory mechanisms and its role in antibacterial, antiviral and some inflammatory diseases.<sup>5</sup> By the mouse model of partial hepatic IR injury, we verified that OI, that is, itaconate, can markedly attenuate liver IR insult, as shown by the reduction in transaminase levels, decrease in inflammatory cytokine release, alleviation of liver tissue insult and inhibition of hepatocyte apoptosis. These results demonstrated the protective

effect of itaconate in hepatic IR injury through its anti-inflammation, antioxidative and antiapoptotic effects. Even though the mainstream research on liver IR injury focuses on hepatocytes, more and more studies have reported that nonparenchymal cells were indispensable in this process.<sup>2-4</sup> Yi et al revealed that itaconate have a hepatocyte-specific protective effect by activating Nrf2-driven signaling in liver IR injury,<sup>9</sup> but it is worth further consideration and research on whether itaconate protects the liver from IR injury through macrophage metabolic remodeling.

Then, we sequenced the RNA from experimental liver tissues and carried out comprehensive bioinformatics analysis. Functional analysis was performed to provide a reference for itaconate-mediated protection and evidence for identifying the corresponding lncRNAs. Intriguingly, the mRNAs that were downregulated after OI pretreatment seemed to better reflect the effect of itaconate and showed high functional consistency with the mRNAs that were upregulated after IR injury. GO analysis indicated that these mRNAs participated in the inflammatory response and immune response, involving multiple inflammatory

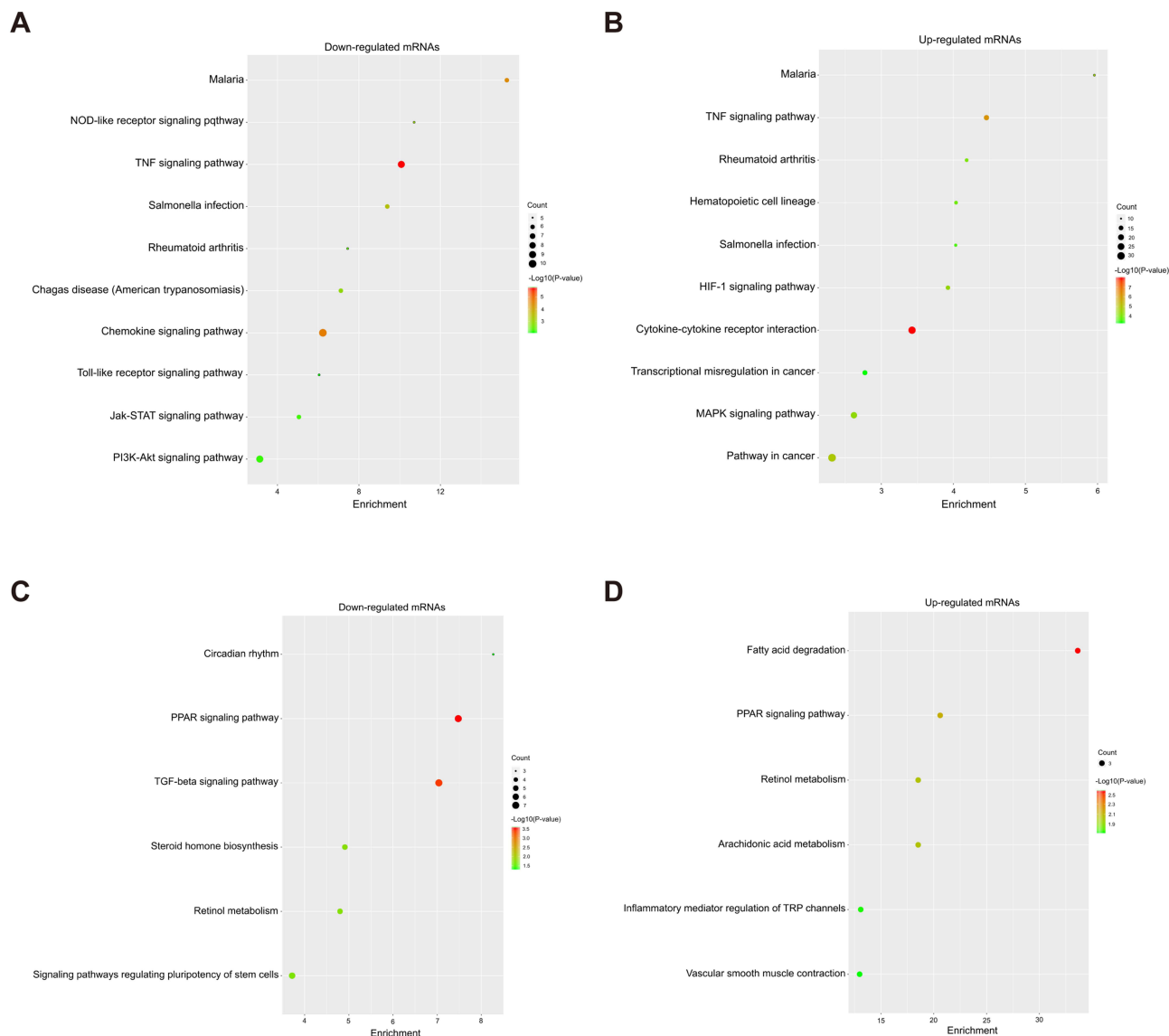


**Figure 6** KEGG analysis of significantly differentially expressed genes. KEGG pathways of upregulated and downregulated mRNAs in the IR Con vs Sham Con group and the IR OI vs IR Con group. **(A)** Downregulated mRNAs after OI pretreatment. **(B)** Upregulated mRNAs after hepatic IR injury. **(C)** Downregulated mRNAs after hepatic IR injury. **(D)** Upregulated mRNAs after OI pretreatment. The top ten or all the pathways with  $P < 0.05$  were listed.

**Abbreviations:** KEGG, Kyoto Encyclopedia of Genes and Genomes; mRNAs, messenger RNAs; IR, ischemia-reperfusion; OI, 4-octyl itaconate.

cells and immune cells together with multiple cytokines and chemokines. These results are consistent with what we know about the pathophysiological mechanism of liver IR injury.<sup>2,27,28</sup> In addition, KEGG analysis revealed some interrelated pathways of liver IR injury, including the TNF signaling pathway,<sup>29,30</sup> NOD (nucleotide oligomerization domain)-like receptor signaling pathway,<sup>31</sup> chemokine signaling pathway,<sup>32</sup> Toll-like receptor signaling pathway,<sup>33,34</sup> and PI3K (phosphatidylinositol 3 kinase)-Akt signaling pathway,<sup>35,36</sup> which also suggested that

these signaling pathways might be involved in the protective effect of itaconate.

Furthermore, we focused on 41 mRNAs that were markedly differentially expressed only in two comparison groups and exhibited the exact opposite trends in expression in these groups. As mentioned above, most of these mRNAs were upregulated in the IR Con vs Sham Con group and downregulated in the IR OI vs IR Con group. We performed PPI network analysis of these mRNAs and identified one key gene cluster that consisted of eight

**Table 5** 14 Identical Pathways in Both the IR Con vs Sham Con and the IR OI vs IR Con Group

KEGG Pathways	IR Con vs Sham Con		IR OI vs IR Con	
	Count	P-value	Count	P-value
TNF signaling pathway	17	9.79E-07	9	2.25E-06
Chemokine signaling pathway	15	0.008420059	10	2.38E-05
Malaria	10	3.37E-05	6	3.79E-05
Salmonella infection	11	3.46E-04	6	3.88E-04
NOD-like receptor signaling pathway	8	0.003434381	5	0.001098843
Chagas disease (American trypanosomiasis)	10	0.009535324	6	0.001380861
Rheumatoid arthritis	12	1.17E-04	5	0.004188718
PI3K-Akt signaling pathway	25	0.001160169	9	0.006804498
Toll-like receptor signaling pathway	9	0.024256493	5	0.008729861
Legionellosis	8	0.003434381	4	0.010716493
Pertussis	7	0.043575921	4	0.021562541
Hematopoietic cell lineage	12	1.62E-04	4	0.030878788
African trypanosomiasis	6	0.006820615	3	0.032081657
Influenza A	12	0.0363439	5	0.048605997

**Abbreviations:** IR, ischemia-reperfusion; OI, 4-octyl itaconate; KEGG, Kyoto Encyclopedia of Genes and Genomes; TNF, tumor necrosis factor; NOD, nucleotide oligomerization domain; PI3K, phosphatidylinositol 3 kinase.

mRNAs (*Il6*, *Il1b*, *Ptgs2*, *Mmp13*, *Ccl3*, *Ccl4*, *Osm* and *Il1f9*). Previous research<sup>37,38</sup> and our study confirmed that proinflammatory cytokines, including IL-6 and IL-1 $\beta$ , are increased during IR injury. Moreover, our results showed that OI pretreatment significantly reduced the levels of these cytokines, and many studies have also demonstrated that itaconate can exert an anti-inflammatory effect by inhibiting the transcription and release of IL-1 $\beta$  and IL-6 in lipopolysaccharide (LPS)-activated macrophages through several mechanisms.<sup>5-7</sup> PTGS2, also known as Cyclooxygenase-2 (COX-2), was greatly expressed after liver IR injury, while COX-2 deficiency alleviated liver damage after IR injury.<sup>39</sup> It was reported that dimethyl fumarate inhibits macrophage activation by enhancing antioxidant function through the Nrf-2 pathway, causing COX-2 protein expression to decrease markedly at the initial stage of liver IR injury.<sup>40</sup> Our results confirmed that OI, which is also an Nrf2 activator,<sup>7</sup> might also play the same role. MMP-13 can promote early liver injury and fibrosis by regulating the expression of proinflammatory mediators, and the expression and processing of connective tissue growth factor (CTGF) and transforming growth factor- $\beta$ 1 (TGF- $\beta$ 1) in mice.<sup>41</sup> Although research on MMP-13 in liver IR injury is not available, a study suggested that MMP-13 is important in IR-related brain injury, and the level of MMP-13 gradually increased with time after cerebral IR and was markedly higher than that in the sham group after 48 hours.<sup>42</sup> CCL3 and CCL4, also

known as macrophage inflammatory protein-1 $\alpha$  (MIP-1 $\alpha$ ) and macrophage inflammatory protein-1 $\beta$  (MIP-1 $\beta$ ), were examined in liver endothelial cells several hours after liver transplantation reperfusion, and they were continuously expressed during acute cellular rejection. It seemed that inhibition of the secretion of these chemokines was one of the mechanisms of the success of corticosteroid therapy for acute rejection.<sup>43</sup> However, *Osm* and *Il1f9* have rarely been studied in IR injury to date.

*Cis* regulation occurs when lncRNAs regulate the adjacent gene expression on the same chromosome or regulate the chromatin status to affect gene transcription.<sup>44</sup> The lncRNA MSTRG.19961, which is located on chromosome 11, might act as a *cis* regulator of *Ccl3* and *Ccl4*, which are located on the same chromosome. Our study showed that both of these genes were downregulated in mice pretreated with itaconate, while lncRNA MSTRG.19961 was upregulated. Accordingly, itaconate might have a positive regulatory effect on lncRNA MSTRG.19961. Itaconate, as an Nrf2 activator, plays a hepatoprotective role during liver IR injury by activating Nrf2 antioxidative response in hepatocytes.<sup>8</sup> So far, the regulatory relationship between *Ccl3* or *Ccl4* and *Nrf2* has not been studied in liver IR injury. Whereas the mRNA level of *Ccl3* was significantly increased in cerebral hypoperfusion mice; similarly, the mRNA level of *Ccl3* increased significantly in *Nrf2*<sup>-/-</sup> hypoperfused mice compared with sham mice.<sup>45</sup> Dimethyl fumarate, an Nrf2-activating drug, can

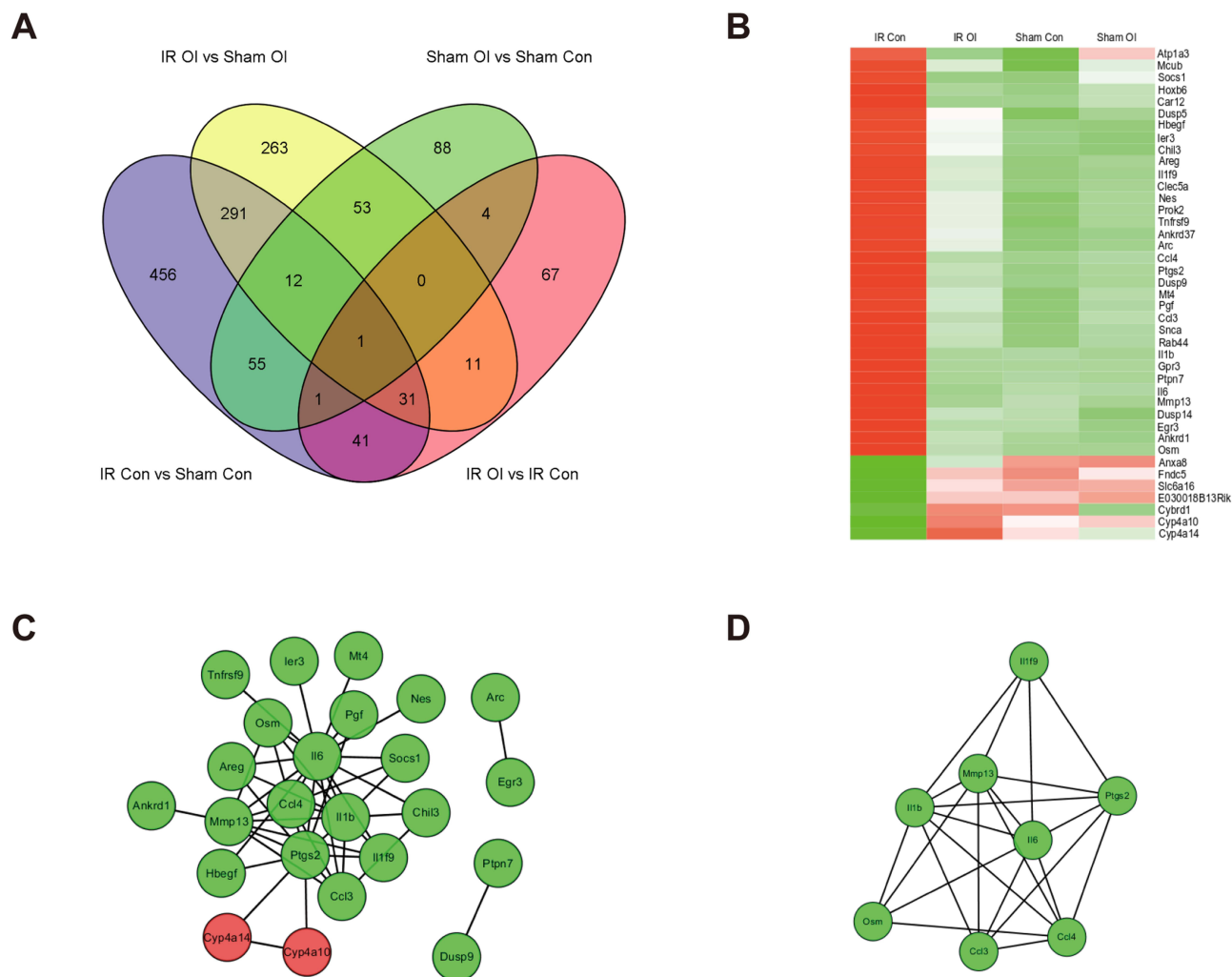


**Figure 7** PPI network and significant gene cluster of selected mRNAs. **(A)** Venn diagram was used to demonstrate the counts of unique or common mRNAs among diverse comparison groups. **(B)** Heatmap shows the expression of 41 mRNAs that were significantly differentially expressed only after hepatic IR injury and after OI pretreatment. The color scale represents the variation of expression. Red indicates upregulation and green indicates downregulation. **(C)** 41 genes were filtered (combined score > 0.4) into the PPI network including 24 nodes and 46 edges. **(D)** One key gene cluster of eight mRNAs was identified by the plugin “MCODE”. Red represents upregulated mRNA and green represents downregulated mRNA.

**Abbreviations:** PPI, protein-protein interaction; mRNAs, messenger RNAs; IR, ischemia-reperfusion; OI, 4-octyl itaconate; MCODE, Molecular Complex Detection.

dampen the levels of CCL3,<sup>46</sup> a synthetic oleanolic triterpenoid that appears to be potent activator of Nrf2 suppressed the expression of CCL4.<sup>47</sup> Our qRT-PCR results showed that the increase of MSTRG.19961 expression in the IR OI vs IR Con group was not very high, however. As potential candidate genes, whether *Ccl3* or *Ccl4* involves Nrf2 dependent hepatoprotection by itaconate or they are regulated by MSTRG.19961 needs further verification. In addition, lncRNAs regulate the expression of distant genes through a *trans*-acting mechanism.<sup>44</sup> A total of 413 lncRNA-mRNA pairs that may have direct regulatory relationship were identified. All of these results demonstrated the potential protective effect of itaconate on liver IR injury, and these lncRNA-mRNA pairs could be good

alternatives for studying the mechanism by which itaconate ameliorates liver IR injury.

## Conclusion

In summary, our study confirmed that itaconate can protect the liver from IR injury in mice and used RNA-Seq and bioinformatics analysis to identify lncRNAs relevant to this itaconate-mediated protection. Although this work is only preliminary and further experimental verification is needed, this is a breakthrough study that provides a completely new understanding of the mechanism by which itaconate affects liver IR injury and exerts its anti-inflammatory and antioxidative stress effects.

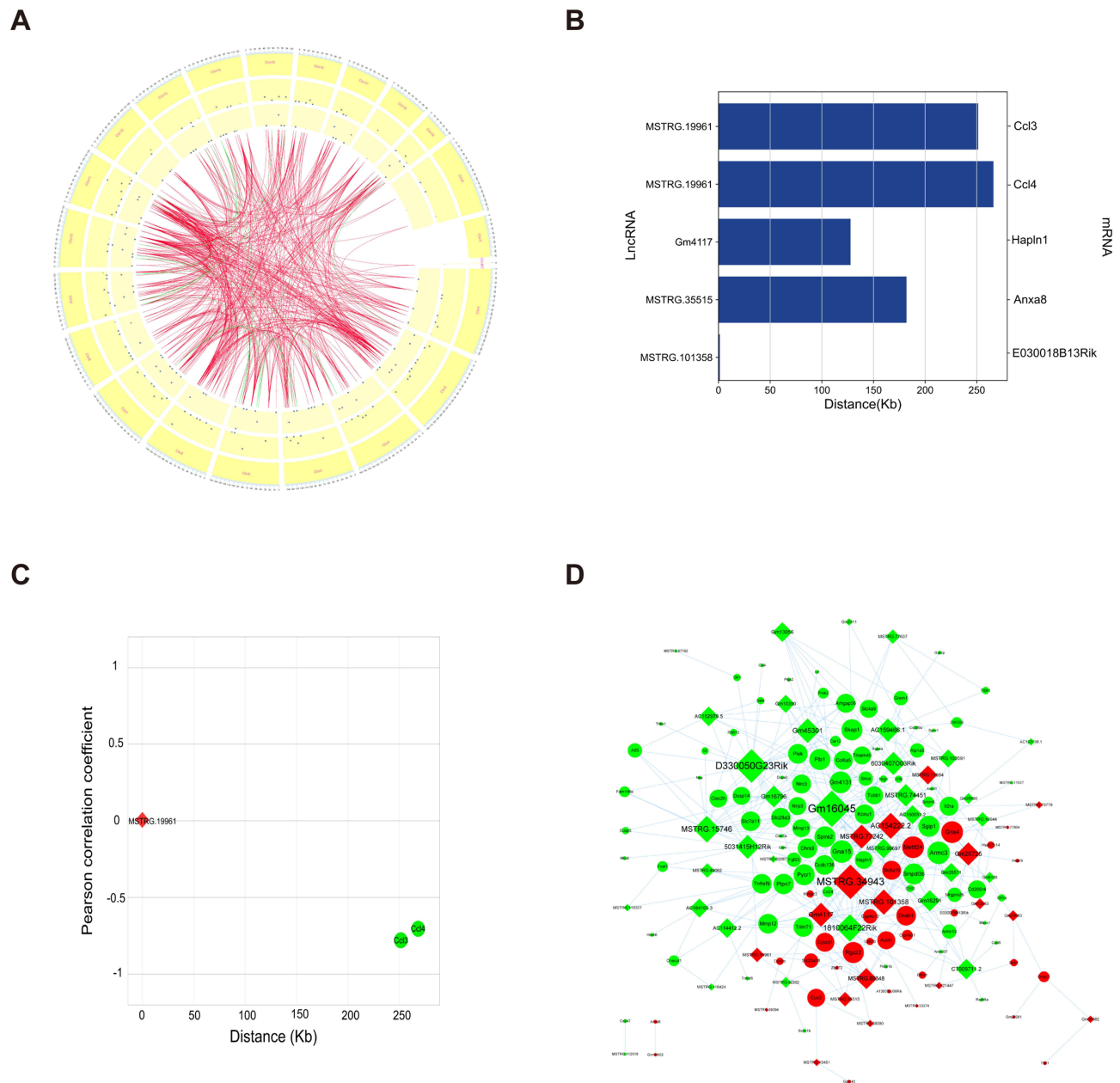


**Figure 8** *Cis* and *trans* regulatory mechanism of lncRNAs. **(A)** The coexpressed lncRNA-mRNA pairs ( $PCC \geq 0.70$  and  $P < 0.05$ ) are displayed by the Circos diagram. The outer ring shows the distribution of the chromosomes of the mouse; the middle circle shows the distribution of markedly differentially expressed mRNAs and the inner ring shows the distribution of differentially expressed lncRNAs. The internal lines indicate that the top 500 lncRNA-mRNA pairs. Green line indicates negative correlation and red line indicates positive correlation. **(B)** Five pairs of *cis*-regulated lncRNAs and mRNAs. Left and right of the ordinate are lncRNA and mRNA, respectively; the abscissa shows the distance between mRNA and lncRNA. **(C)** lncRNA MSTRG.19961 regulates *Ccl3* and *Ccl4* in *cis*. The abscissa shows the distance between the mRNA and lncRNA. The ordinate shows the PCC between the mRNA and lncRNA. **(D)** lncRNA-mRNA network reflected *trans* regulatory function of lncRNAs. Red diamond indicates upregulated lncRNA and green diamond indicates downregulated lncRNA. Red ellipse indicates upregulated mRNA and green ellipse indicates downregulated mRNA. The node size represents the number of lncRNA-mRNA pairs.

**Abbreviations:** lncRNAs, long non-coding RNAs; mRNA, messenger RNA; PCC, Pearson correlation coefficient; *Ccl3*, chemokine (C-C motif) ligand 3; *Ccl4*, chemokine (C-C motif) ligand 4.

## Abbreviations

lncRNAs, long non-coding RNAs; IR, ischemia-reperfusion; OI, 4-octyl itaconate; RNA-Seq, RNA sequencing; mRNAs, messenger RNAs; PPI, protein-protein interaction; SDH,

succinate dehydrogenase; IL-1 $\beta$ , interleukin 1 $\beta$ ; HIF-1 $\alpha$ , hypoxia inducible factor-1 $\alpha$ ; Nrf2, nuclear factor E2-related factor 2; KEAP1, kelch-like ECH-associated protein 1; HOTAIR, HOX transcript antisense RNA; ATG7, autophagy

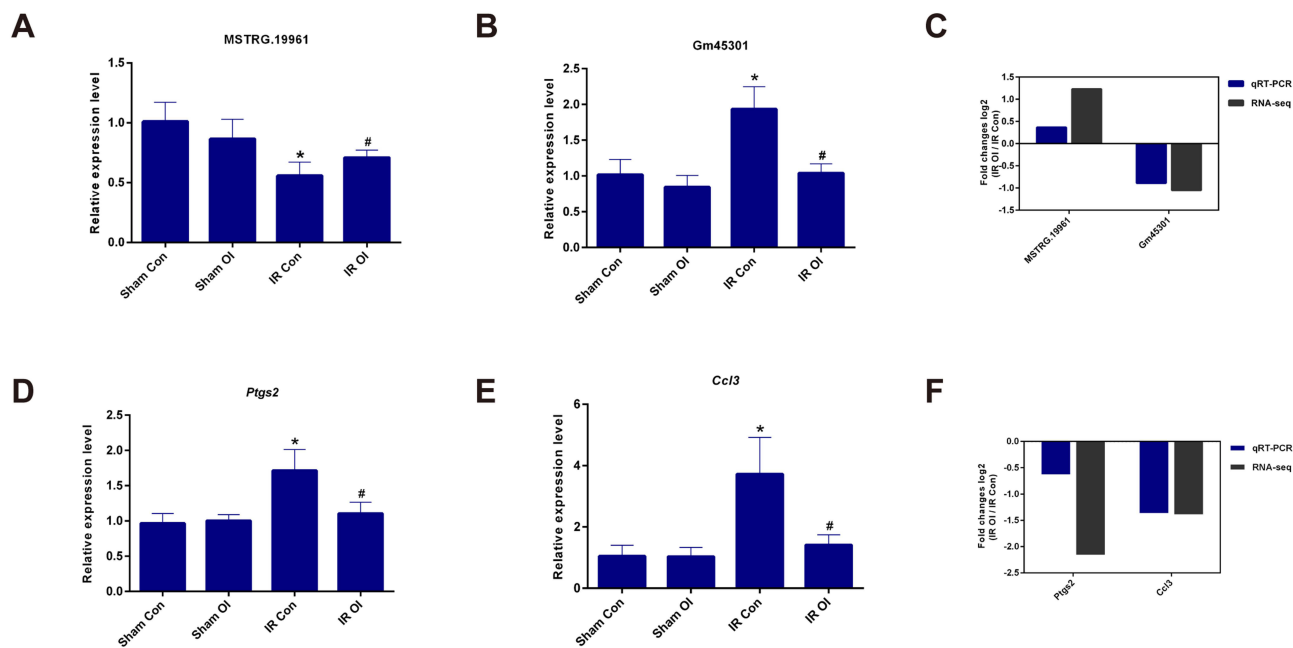


**Figure 9** Validation for selected lncRNAs and mRNAs by real-time qRT-PCR. (A and B) The relative expression levels of two lncRNAs were detected in four comparison groups. (C) The log<sub>2</sub>-transformed fold change values were compared between qRT-PCR results and RNA-seq data in the IR OI vs IR Con group. (D and E) The relative expression levels of two mRNAs were detected in four comparison groups. (F) The log<sub>2</sub>-transformed fold change values were compared between qRT-PCR results and sequencing data in the IR OI vs IR Con group. Each group has five samples. Data are shown as mean ± SD of three independent experiments performed in triplicate. \*Significant difference from the Sham Con group, P < 0.05. #Significant difference from the IR Con group, P < 0.05. **Abbreviations:** lncRNAs, long non-coding RNAs; mRNAs, messenger RNAs; qRT-PCR, quantitative reverse transcription polymerase chain reaction; RNA-Seq, RNA sequencing; IR, ischemia-reperfusion; OI, 4-octyl itaconate; SD, standard deviation; *Ptgs2*, prostaglandin-endoperoxide synthase 2; *Ccl3*, chemokine (C-C motif) ligand 3; *Gapdh*, glyceraldehyde-3-phosphate dehydrogenase.

related 7; MEG3, maternally expressed gene 3; NF-κB, nuclear transcription factor kappa B; SPF, specific pathogen-free; ALT, alanine aminotransferase; AST, aspartate aminotransferase; TNF-α, tumor necrosis factor-α; IL-6, interleukin 6; ELISA, enzyme linked immunosorbent assay; TUNEL, Terminal dUTP nick-end labeling; GO, Gene Ontology; KEGG, Kyoto Encyclopedia of Genes and Genomes; DAVID, Database for Annotation, Visualization and Integrated Discovery; STRING, Search Tool for the Retrieval of Interacting Genes; MCODE, Molecular Complex Detection; PCC, Pearson correlation coefficient; qRT-PCR, quantitative reverse transcription polymerase chain reaction; *Gapdh*, Glyceraldehyde 3-phosphate dehydrogenase; SD, standard deviation; HE, hematoxylin-eosin; *Il6*, interleukin 6; *Il1b*, interleukin 1 beta; *Ptgs2*, prostaglandin-endoperoxide synthase 2; *Mmp13*, matrix metalloproteinase 13; *Ccl3*, chemokine (C-C motif) ligand 3; *Ccl4*, chemokine (C-C motif) ligand 4; *Osm*, oncostatin M; *Il1f9*, interleukin 1 family, member 9; NOD, nucleotide oligomerization domain; PI3K, phosphatidylinositol 3 kinase; LPS, lipopolysaccharide; COX-2, Cyclooxygenase-2; CTGF, connective tissue growth factor; TGF-β1, transforming growth

factor-β1; MIP-1α, macrophage inflammatory protein-1α; MIP-1β, macrophage inflammatory protein-1β; FC, fold change; *Hsd17b14*, hydroxysteroid (17-beta) dehydrogenase 14; *Mesp2*, mesoderm posterior 2; *Mybpc3*, myosin binding protein C3; *Cux2*, cut-like homeobox 2; *Anxa8*, annexin A8; *Ccl19*, chemokine (C-C motif) ligand 19; *Chrne*, cholinergic receptor, nicotinic, epsilon polypeptide; *Grem1*, gremlin 1; DAPI, 4',6-diamidino-2-phenylindole; BP, biological process; CC, cellular component; MF, molecular function.

### Data Sharing Statement

The raw data of RNA-seq were deposited in NCBI Sequence Read Archive with accession number PRJNA702236.

### Acknowledgments

This work was supported by grants from the Outstanding Youth Training Fund from Academician Yu Weihao of Harbin Medical University (2014), Scientific Foundation of the First Affiliated Hospital of Harbin Medical University (2019L01, HYD2020JQ0007), Heilongjiang Postdoctoral Foundation (LBH-Z11066), China



Postdoctoral Science Foundation (2012M510990, 2013T60387), Natural Science Foundation of Heilongjiang Province of China (LC2018037) and the National Natural Scientific Foundation of China (81100305, 81470876 and 81270527).

## Author Contributions

All authors made substantial contributions to conception and design, acquisition of data, or analysis and interpretation of data; took part in drafting the article or revising it critically for important intellectual content; agreed to submit to the current journal; gave final approval of the version to be published; and agree to be accountable for all aspects of the work.

## Disclosure

The authors report no conflicts of interest in this work.

## References

- Zhai Y, Petrowsky H, Hong JC, Busuttill RW, Kupiec-Weglinski JW. Ischaemia-reperfusion injury in liver transplantation—from bench to bedside. *Nat Rev Gastroenterol Hepatol*. 2013;10(2):79–89.
- Lu TF, Yang TH, Zhong CP, et al. Dual effect of hepatic macrophages on liver ischemia and reperfusion injury during liver transplantation. *Immune Netw*. 2018;18(3):e24.
- Sun YY, Li XF, Meng XM, Huang C, Zhang L, Li J. Macrophage phenotype in liver injury and repair. *Scand J Immunol*. 2017;85(3):166–174.
- Konishi T, Lentsch AB. Hepatic ischemia/reperfusion: mechanisms of tissue injury, repair, and regeneration. *Gene Expr*. 2017;17(4):277–287.
- Hooftman A, O'Neill LAJ. The immunomodulatory potential of the metabolite itaconate. *Trends Immunol*. 2019;40(8):687–698.
- Lampropoulou V, Sergushichev A, Bambouskova M, et al. Itaconate links inhibition of succinate dehydrogenase with macrophage metabolic remodeling and regulation of inflammation. *Cell Metab*. 2016;24(1):158–166.
- Mills EL, Ryan DG, Prag HA, et al. Itaconate is an anti-inflammatory metabolite that activates Nrf2 via alkylation of KEAP1. *Nature*. 2018;556(7699):113–117.
- Zheng Y, Chen Z, She C, et al. Four-octyl itaconate activates Nrf2 cascade to protect osteoblasts from hydrogen peroxide-induced oxidative injury. *Cell Death Dis*. 2020;11(9):772.
- Yi Z, Deng M, Scott MJ, et al. Immune-responsive gene 1/itaconate activates nuclear factor erythroid 2-related factor 2 in hepatocytes to protect against liver ischemia-reperfusion injury. *Hepatology*. 2020;72(4):1394–1411.
- Tang B, Bao N, He G, Wang J. Long noncoding RNA HOTAIR regulates autophagy via the miR-20b-5p/ATG7 axis in hepatic ischemia/reperfusion injury. *Gene*. 2019;686:56–62.
- Huang X, Gao Y, Qin J, Lu S. The mechanism of long non-coding RNA MEG3 for hepatic ischemia-reperfusion: mediated by miR-34a/Nrf2 signaling pathway. *J Cell Biochem*. 2018;119(1):1163–1172.
- Chen Z, Jia S, Li D, et al. Silencing of long noncoding RNA AK139328 attenuates ischemia/reperfusion injury in mouse livers. *PLoS One*. 2013;8(11):e80817.
- Dai B, Qiao L, Zhang M, et al. lncRNA AK054386 functions as a ceRNA to sequester miR-199 and induce sustained endoplasmic reticulum stress in hepatic reperfusion injury. *Oxid Med Cell Longev*. 2019;2019:8189079.
- Chen Q, Meng X, Liao Q, Chen M. Versatile interactions and bioinformatics analysis of noncoding RNAs. *Brief Bioinform*. 2019;20(5):1781–1794.
- Chen Z, Luo Y, Yang W, et al. Comparison analysis of dysregulated lncRNA profile in mouse plasma and liver after hepatic ischemia/reperfusion injury. *PLoS One*. 2015;10(7):e0133462.
- ElAZzouny M, Tom CT, Evans CR, et al. Dimethyl itaconate is not metabolized into itaconate intracellularly. *J Biol Chem*. 2017;292(12):4766–4769.
- Wang D, Ma Y, Li Z, et al. The role of AKT1 and autophagy in the protective effect of hydrogen sulphide against hepatic ischemia/reperfusion injury in mice. *Autophagy*. 2012;8(6):954–962.
- Pan S, Liu L, Pan H, et al. Protective effects of hydroxytyrosol on liver ischemia/reperfusion injury in mice. *Mol Nutr Food Res*. 2013;57(7):1218–1227.
- Wang C, Li Z, Zhao B, et al. PGC-1 $\alpha$  protects against hepatic ischemia reperfusion injury by Activating PPAR $\alpha$  and PPAR $\gamma$  and regulating ROS production. *Oxid Med Cell Longev*. 2021;2021:6677955.
- Ashburner M, Ball CA, Blake JA, et al. Gene ontology: tool for the unification of biology. The Gene Ontology Consortium. *Nat Genet*. 2000;25(1):25–29.
- Kanehisa M, Goto S. KEGG: Kyoto encyclopedia of genes and genomes. *Nucleic Acids Res*. 2000;28(1):27–30.
- Dennis G Jr, Sherman BT, Hosack DA, et al. DAVID: database for annotation, visualization, and integrated discovery. *Genome Biol*. 2003;4(5):P3.
- Szklarczyk D, Franceschini A, Kuhn M, et al. The STRING database in 2011: functional interaction networks of proteins, globally integrated and scored. *Nucleic Acids Res*. 2011;39(DatabaseIssue):D561–D568.
- Shannon P, Markiel A, Ozier O, et al. Cytoscape: a software environment for integrated models of biomolecular interaction networks. *Genome Res*. 2003;13(11):2498–2504.
- Chen C, Chen H, Zhang Y, et al. TBtools: an integrative toolkit developed for interactive analyses of big biological data. *Mol Plant*. 2020;13(8):1194–1202.
- Alkan F, Wenzel A, Palasca O, et al. Rsearch2: suffix array-based large-scale prediction of RNA-RNA interactions and siRNA off-targets. *Nucleic Acids Res*. 2017;45(8):e60.
- Caldwell CC, Tschoep J, Lentsch AB. Lymphocyte function during hepatic ischemia/reperfusion injury. *J Leukoc Biol*. 2007;82(3):457–464.
- Mukhopadhyay P, Horváth B, Zsengeller Z, et al. Mitochondrial reactive oxygen species generation triggers inflammatory response and tissue injury associated with hepatic ischemia-reperfusion: therapeutic potential of mitochondrially targeted antioxidants. *Free Radic Biol Med*. 2012;53(5):1123–1138.
- Kim SJ, Eum HA, Billiar TR, Lee SM. Role of heme oxygenase 1 in TNF/TNF receptor-mediated apoptosis after hepatic ischemia/reperfusion in rats. *Shock*. 2013;39(4):380–388.
- Li SP, Wang FF, Zhang WK, et al. Characteristics of changes in inflammatory cytokines as a function of hepatic ischemia-reperfusion injury stage in mice. *Inflammation*. 2019;42(6):2139–2147.
- Xu T, Du Y, Fang XB, et al. New insights into Nod-like receptors (NLRs) in liver diseases. *Int J Physiol Pathophysiol Pharmacol*. 2018;10(1):1–16.
- Zheng J, Li H, He L, et al. Preconditioning of umbilical cord-derived mesenchymal stem cells by rapamycin increases cell migration and ameliorates liver ischaemia/reperfusion injury in mice via the CXCR4/CXCL12 axis. *Cell Prolif*. 2019;52(2):e12546.
- Chang WJ, Toledo-Pereyra LH. Toll-like receptor signaling in liver ischemia and reperfusion. *J Invest Surg*. 2012;25(4):271–277.
- Mahmoud MF, Gamal S, El-Fayoumi HM. Limonin attenuates hepatocellular injury following liver ischemia and reperfusion in rats via toll-like receptor dependent pathway. *Eur J Pharmacol*. 2014;740:676–682.

35. Ke B, Shen XD, Ji H, et al. HO-1-STAT3 axis in mouse liver ischemia/reperfusion injury: regulation of TLR4 innate responses through PI3K/PTEN signaling. *J Hepatol.* 2012;56(2):359–366.
36. Li Z, Zhao F, Cao Y, et al. DHA attenuates hepatic ischemia reperfusion injury by inhibiting pyroptosis and activating PI3K/Akt pathway. *Eur J Pharmacol.* 2018;835:1–10.
37. The DO, Marques PE, Poosti F, et al. Intravital microscopic evaluation of the effects of a CXCR2 antagonist in a model of liver ischemia reperfusion injury in mice. *Front Immunol.* 2017;8:1917.
38. Yue S, Zhu J, Zhang M, et al. The myeloid heat shock transcription factor 1/ $\beta$ -catenin axis regulates NLR family, pyrin domain-containing 3 inflammasome activation in mouse liver ischemia/reperfusion injury. *Hepatology.* 2016;64(5):1683–1698.
39. Hamada T, Tsuchihashi S, Avanesyan A, et al. Cyclooxygenase-2 deficiency enhances Th2 immune responses and impairs neutrophil recruitment in hepatic ischemia/reperfusion injury. *J Immunol.* 2008;180(3):1843–1853.
40. Takasu C, Vaziri ND, Li S, et al. Treatment with dimethyl fumarate ameliorates liver ischemia/reperfusion injury. *World J Gastroenterol.* 2017;23(25):4508–4516.
41. George J, Tsutsumi M, Tsuchishima M. MMP-13 deletion decreases profibrogenic molecules and attenuates N-nitrosodimethylamine-induced liver injury and fibrosis in mice. *J Cell Mol Med.* 2017;21(12):3821–3835.
42. Chen X, Patra A, Sadowska GB, Stonestreet BS. Ischemic-reperfusion injury increases matrix metalloproteinases and tissue metalloproteinase inhibitors in fetal sheep brain. *Dev Neurosci.* 2018;40(3):234–245.
43. Adams DH, Hubscher S, Fear J, Johnston J, Shaw S, Afford S. Hepatic expression of macrophage inflammatory protein-1 alpha and macrophage inflammatory protein-1 beta after liver transplantation. *Transplantation.* 1996;61(5):817–825.
44. Kopp F, Mendell JT. Functional classification and experimental dissection of long noncoding RNAs. *Cell.* 2018;172(3):393–407.
45. Sigfridsson E, Marangoni M, Hardingham GE, Horsburgh K, Fowler JH. Deficiency of Nrf2 exacerbates white matter damage and microglia/macrophage levels in a mouse model of vascular cognitive impairment. *J Neuroinflammation.* 2020;17(1):367.
46. Fowler JH, McQueen J, Holland PR, et al. Dimethyl fumarate improves white matter function following severe hypoperfusion: involvement of microglia/macrophages and inflammatory mediators. *J Cereb Blood Flow Metab.* 2018;38(8):1354–1370.
47. Li B, Abdalrahman A, Lai Y, et al. Dihydro-CDDO-trifluoroethyl amide suppresses inflammatory responses in macrophages via activation of Nrf2. *Biochem Biophys Res Commun.* 2014;444(4):555–561.

## Journal of Inflammation Research

Dovepress

### Publish your work in this journal

The Journal of Inflammation Research is an international, peer-reviewed open-access journal that welcomes laboratory and clinical findings on the molecular basis, cell biology and pharmacology of inflammation including original research, reviews, symposium reports, hypothesis formation and commentaries on: acute/chronic inflammation; mediators of inflammation; cellular processes; molecular

mechanisms; pharmacology and novel anti-inflammatory drugs; clinical conditions involving inflammation. The manuscript management system is completely online and includes a very quick and fair peer-review system. Visit <http://www.dovepress.com/testimonials.php> to read real quotes from published authors.

Submit your manuscript here: <https://www.dovepress.com/journal-of-inflammation-research-journal>